

THE PURIFICATION AND CHARACTERIZATION OF USP30

by

Jason Cargill

A thesis submitted to the Faculty of the University of Delaware in partial fulfillment of the requirements for the degree of Master of Science in Chemistry and Biochemistry

Summer 2017

© 2017 Jason Cargill
All Rights Reserved

THE PURIFICATION AND CHARACTERIZATION OF USP30

by

Jason Cargill

Approved: _____
Zihao Zhuang, Ph.D.
Professor in charge of thesis on behalf of the Advisory Committee

Approved: _____
Murray V. Johnston, Ph.D.
Chair of the Department of Chemistry and Biochemistry

Approved: _____
George H. Watson, Ph.D.
Dean of the College of Arts and Sciences

Approved: _____
Ann L. Ardis, Ph.D.
Senior Vice Provost for Graduate and Professional Education

ACKNOWLEDGMENTS

I would first like to thank my advisor Dr. Zhihao Zhuang. Dr. Zhuang has supported my growth as a scientist through his advice and example. He taught me that integrity is both a scientist highest virtue and greatest asset. Thank you for never giving up on me.

I am completely indebted to my amazing family for their support and encouragement. My parents Jim and Joan Cargill who continue to show me the meaning of sacrifice. I could not manage without my wonderful wife Dani Cargill who put up with my late nights and uneven temperament. I would also like to thank my friend Vaughn for the inspiration he provided.

I would like to thank my lab mates for their suggestion and guidance. Especially Christine Ott, Kun Yang, Ping Gong, Aditi Khankhoje, Guorui Li, Weijun Gui, Prajwal Paudel, Gregory Davidson, and Rosemary Flores.

Last but not least like to thank my committee members and professors that guided me: Dr. Sandeep Patel, Dr. Cecilia Arighi, Dr. Junghuei Chen, Dr. Jon Koh, and Dr. Hal White.

TABLE OF CONTENTS

LIST OF FIGURES	v
ABSTRACT	vii
Chapter	
1 INTRODUCTION	1
2 RESULTS	7
2.1 Cloning	7
2.2 Protein Expression	12
2.3 Protein Purification	13
2.4 Kinetics	17
3 MATERIALS AND METHODS	21
3.1 DNA Purification	21
3.2 pET-15b USP30 Vector Creation	21
3.3 Site directed mutagenesis	23
3.4 Transformation Procedure	24
3.5 Sequencing	24
3.6 Expression test	24
3.7 BL21(DE3) cell cultivation and harvesting	25
3.8 Stage 1 purification	25
3.9 Stage 2 Purification	26
3.10 Stage 3 Purification	26
3.11 UB-AMC production	27
3.12 Kinetics	28
4 DISCUSSION	29
REFERENCES	32

LIST OF FIGURES

- Figure 1 **USP30-SUMO Affinity Purification.** SDS-PAGE analysis of purification using Ni-NTA resin to isolate the His tagged SUMO USP30 protein. The bands in the imidazole elution fraction near 66.4 kDa are SUMO-USP30. The expressed truncated USP30-SUMO can be seen close to 20 kDa. 8
- Figure 2 **USP30 Ion Exchange Chromatography:** Top Image: SDS-PAGE page of USP30 separation from SUMO using anion exchange. There is a clear separation between the proteins but a portion of the USP30 can be seen to overlap the SUMO fractions. Bottom Image: Shows the chromatogram of the ion exchange chromatography. 9
- Figure 3 **pET-15b Cloning-Expression Region:** Amino acid sequence translated from DNA sequence results. The His tag is represented in green, the TEV cleavage site is yellow, USP30 sequence is show in blue. 10
- Figure 4 **PCR Amplification Result:** Agarose gel image of the PCR reaction visualized using ethidium bromide. The amplification band is located at the expected length for the 1386 bp USP30 gene. 10
- Figure 5 **Double digestion of pET-15b vector:** The first two lanes after the ladder are the single digestion from XhoI and NdeI respectively. The fourth lane is the double digested pET-15b vector. The PCNA gene has been excised and can be seen between 1 and 1.5 kbp markers in the ladder. ... 11
- Figure 6 **Gene insertion verification via PCR amplification:** To screen for colonies with the targeted gene inserted, a PCR reaction was performed using primers that would only amplify the USP30 gene. A control of unreacted mixture was run on the gel. Colonies 6, 9, and 11 show a positive result. 12
- Figure 7 **BL21(DE3) Cells Expression Test:** BL21(DE3) cells transformed with the pET-15b vector containing the USP30 gene were induced using either 0.4 mM or 1 mM IPTG. Samples were taken at various times and analyzed. 13

Figure 8 Analysis of affinity chromatography: Gel analysis shows a strong band of the target protein after induction. The presence of the target protein in the pellet fraction indicates some of the expressed protein was insoluble along with a major contaminating band. The flow through and wash fractions are relatively free of target protein indicating tight binding between the affinity beads and the target protein. Imidazole elution fractions show a relatively pure sample with an impurity above the target protein.....	15
Figure 9 Cation Exchange Chromatography: Impurities that previously bound to the Ni-NTA resin had the property of carrying a net negative charge. By using a cation exchange column in the next step, many of the impurities did not bind to the column and were present in the flow through fractions.....	15
Figure 10 Final SDS-PAGE analysis of purified USP30 protein: The resulting protein of the three chromatography methods shows high purity at a concentration of 14 mg/ml.	17
Figure 11 Lineweaver-Burk Analysis of Wild Type USP30: Analysis based on the Ub-AMC cleavage fluorescence rate. A k_{cat}/K_M value of $2.26 \times 10^4 \text{ M}^{-1} \text{ s}^{-1}$ was determined.	19
Figure 12 USP30 Active Site Mutant Purity Assesd SDS –PAGE: The purity of the mutant (C77A), (H452Q), (S477A), and (S477D) is represented in the gel.	20

ABSTRACT

Parkinson is the second most prevalent neurological disorder behind Alzheimer's, affecting over 1 million Americans a year. The disintegration of dopamine producing neural cells in the substantia nigra is the apparent cause of Parkinson. However, the underlying mechanism of impairment is still not well understood. Currently, the most common medications prescribed to Parkinson's patients only treat the symptoms of dopamine loss, either by mimicking dopamine or by altering dopamine levels. These medications do nothing to regress the disease itself. A line of research that would lead to a treatment of the underlying mechanism is much needed. Mounting research points in the direction of mitochondria malfunction as a key factor in the development of Parkinson's. The ubiquitin specific protease USP30 plays a significant role in the management of healthy mitochondria, by acting to regulate the destruction of damaged mitochondrion. A knockdown of the USP30 gene has been shown to alleviate Parkinson's symptoms in flies with parkin mutation. Other promising studies suggest that the USP30 enzyme would be a good target for potential inhibitor studies. However few studies have been performed on the isolated protein itself. In this study, we attempt to close that gap by developing a method to purify large quantities of the enzyme to be used in inhibitor studies and for x ray crystallography. Further evidence for the potential of inhibitor studies is the unique catalytic triad of USP30 (Cys-Asp-Ser). To gain a better understanding of the active site, which could be exploited when developing an inhibitor, we prepared and characterized individual mutants of each of the three amino acids.

Chapter 1

INTRODUCTION

There are an estimated 10 million cases of Parkinson's in the world today, with 60,000 new cases occurring every year in the US¹. The monetary cost of the disorder is upwards of 14.4 Billion dollars per year for United States tax payers alone². Adding to the challenge, Parkinson's can only be diagnosed through indirect methods, which makes early intervention problematic and increases care cost. Despite being the most common movement disorder, knowledge of the pathogenesis of the disease is still deficient. What is known about the disease is that the symptoms stem from a loss of the dopamine producing neurons found in the substantia nigra pars compacta located in the mid brain³. Cases of Parkinson's linked solely to inherited genetic defect are rare. Most cases are spontaneous and are believed to be a combination of environmental and genetic predisposition with environmental factors contributing to 2/3 of the cases⁴.

Current research provides evidence for several contributors to Parkinson's. The most heavily studied contributor to Parkinson's is protein aggregation. As with Alzheimer's disease, the suspected antecedent may be the formation of Lewy Bodies composed of misfolded α -synuclein⁵. This pathology is also able to spread through the transport of α -synuclein from cell to cell⁶. It can be showed that mutant α -synuclein could damage neurons in Midbrain dopaminergic cell cultures⁷. The E3 ligase parkin potentially plays an major role in the regulation of Lewy Body

formation. Overexpression of parkin is capable of reducing the proteasome inhibiting effects of increased α -synuclein production.⁸

The role of the endoplasmic reticulum in protein aggregation is also gaining attention. The cell's reaction to misfolded proteins is the initiation of the endoplasmic reticulum's unfolded protein response (UPR). This response will stop new protein production as well as produce molecular chaperones⁹. If activated for prolonged periods, the UPR will further activate downstream cellular process, which leads to apoptosis¹⁰. Neuronal cells are particularly reliant on the UPR as they rarely divide. Rapidly dividing cells allow for the dilution of misfolded proteins negating the impact of mutated proteins¹¹.

One of the most promising lines of Parkinson's research is investigation into mitochondrial network health. Mitochondrial dysfunction has been shown to precede other markers of neurodegeneration, punctuating its potential involvement in early pathogenesis¹². Mitochondria function impacts both protein aggregation and ER function¹³. The importance of understanding mitochondrial dysfunction is also underscored by its potential as an early indicator of neurodegeneration. This makes research into mitochondrial dysfunction impactful because it is not only linked to Parkinson's but also its connection to nearly all neurodegenerative disorders¹⁴.

Mitophagy is regulated through ubiquitin signaling. The process of linking ubiquitin with a target molecule is regulated by three enzymes (E1, E2, and E3). E1, the ubiquitin activating enzyme, uses ATP to create a high energy thioester bond. E1 then uses this energy to form a covalent bond between the ubiquitin molecule and the E2 enzyme. The E2 enzyme is known as the ubiquitin conjugating enzyme. The E2 enzyme will then pass on the activated ubiquitin to an E3 ubiquitin ligase. The E3

enzyme aids in the specificity of ubiquitin conjugation either by acting as a scaffold protein for the E2 enzyme and the target protein (RING family) or by passing along the ubiquitin molecule to the target protein through a cysteine residue (HECT family). In the case of mitophagy, parkin acts as the E3 enzyme. Following depolarization, parkin acts to ubiquitinate dozens of mitochondrial proteins. Some of the better-studied targets are Mfn1, Mfn2, Miro1, and Tom20.

These proteins are ubiquitinated following depolarization of the outer mitochondrial membrane. Tom20 ubiquitination by parkin has been shown to activate mitophagy¹⁵. Mfn1 and Mfn2 are fusion proteins that are degraded to isolate damaged protein and prevent them from corrupting the network¹⁶. Ubiquitination of Miro1 does not immediately lead to Miro1 turnover, but acts as a signal to block mitochondrial trafficking¹⁷.

The cell's antithesis of ubiquitin ligation is ubiquitin deconjugation. A class of proteases called the deubiquitinases or DUBs for short regulates this process. The human genome codes for over 100 of these DUBs. DUBs consist of six families the ubiquitin C-terminal hydrolases (UCH), Otubain proteases (OTU), Machado-Joseph disease proteases (MJD), JAB/MPN/Mov34 metalloenzymes (JAMM), ubiquitin-specific proteases (USPs), and the newest member motif interacting with Ub-containing novel DUB family (Mindy)¹⁸. Deubiquitinase show specificity to target proteins as well as chain type and length. DUBs function to process and control the level of free ubiquitin in the cell, to edit polyubiquitin chains, and to completely remove ubiquitin from tagged proteins. These enzymes have been shown to be involved in a wide range of functions including DNA damage response, inflammation,

transcription, endosomal sorting and regulating protein levels. USP30 acts as the regulating deubiquitinase for mitophagy.

Mitochondria work in concert to ensure the health of the mitochondrial network. The typical depictions of mitochondria found in eukaryotic cells are that of single free floating organelles. A truer representation is of mitochondria fusing together to form a complex network throughout the cytosol. This network functions to stabilize the distress of any single mitochondrion by spreading out the responsibilities and resources through the whole network. Functional enzymes can be shared with mitochondrion that have misfolded enzymes. This method of protein distribution is so efficient that GFP produced by a single mitochondrion can be seen through out the entirety of the network in one hour¹⁹. The damaged enzymes can also be aggregated and split off from the network into a mitochondrion delivered for degradation through the autophagosome. Senescent mitochondrion and mitochondrion damaged beyond repair are also destined for degradation in the lysosome. This process known as mitophagy is essential to ensure the overall integrity of the mitochondrial network. When this process is hindered, it leads to the failure of the network and eventually the complete cell death.

A poorly functioning mitochondria network has a greater impact on neuronal cells. These cells have more mitochondria than most cells types and require large amounts of energy to function normally. The death of neuronal cells, specifically in the substantia nigra, are known to be correlated with Parkinson's disease. Both mutation in the mitochondrial network-regulating enzymes Pink1 and parkin have been linked to a genetic cause of Parkinson's disease^{20,21}.

Elongated polyubiquitin chains found on the surface of the mitochondria act as the signal to send the tagged organelle to the autophagosome²². Three enzymes, Pink1, parkin, and USP30, working together control the length and abundance of these chains²³.

Pink1 is a outer mitochondria membrane-embedded kinase. The enzyme is recruited to the outer membrane by the translocate of the outer membrane (TOM) complex. Although typically being kept at low levels on the outer membrane of healthy mitochondria, depolarized membranes accumulate high levels of Pink1, which initiates mitophagy of the damaged mitochondrion. Pink1 works to phosphorylate the Serine 65 residue of ubiquitin molecules ligated to the membrane bound proteins in mitochondria²⁴. PINK1 also functions to fully activate parkin by phosphorylating the Serine 65 residue on the ubiquitin-like domain of parkin²⁵.

Parkin, a Ring-between-Ring (RBR) ubiquitin ligase, acts to extend ubiquitin chains found on the surface of proteins embedded in the mitochondria outer membrane. However, in its native state parkin is self-inhibiting. In order to be activated, it must first bind an ubiquitin molecule with an phosphorylated Serine 65. Then parkin's ubiquitin like domain or Ubl domain is made assessable to be phosphorylated on its own Ser65 residue. Parkin is capable of extending multiple chain-linkage types (K48, K63, K11 and K6)²⁶. These extended chains also act as a feedback loop to recruit more parkins, which will further produce polyubiquitin chains.

Deubiquitinases act as the negative regulator of the ubiquitin chain formation in mitochondria. Although both USP35 and USP15 are believed to play a possible role in mitophagy²³, USP30 is the most widely studied mitochondrial deubiquitinase

and has the strongest connection to mitophagy. In order to maintain a healthy mitochondrion homeostasis, USP30 acts as a counter balance to parkin.

Occasionally, when mitochondrion fuse or divide, the membrane will become depolarized. During this period of depolarization, parkin is activated and can act to extend ubiquitin chains; this may lead to unwanted mitophagy. USP30 embedded into the mitochondrial membrane is responsible for returning the ubiquitin signal to normal. However, during prolonged periods of depolarization, which are caused by damage to the membrane, the heavily recruited parkin counteracts USP30 cleavage of polyubiquitin. When mitochondrial membrane depolarization is induced using carbonyl cyanide m-chlorophenyl hydrazone (CCCP) the compound, USP30 overexpression has been shown to delay mitophagy by inhibiting parkin recruitment²⁷. While a USP30 knockdown has been demonstrated to reverse the impaired mitophagy of cells with mutated parkin¹⁷.

Currently all prescribed medication for Parkinson's disease only acts to treat its symptoms but does nothing to alleviate the underlying disorder. A specific inhibitor for USP30 could act to halt and even reverse the effects of mutated parkin. This will, in turn, rescue the damaged mitochondrion network and preserve the neuronal cells. To this end, we seek to understand the function and mechanism of action of USP30 that is linked to mitochondrion homeostasis. Although outside the scope of this thesis, an in-depth understanding of USP30 function and structure may lead to new therapeutics for the Parkinson's disease. My focus in this study is to purify USP30 in an active form and homogeneity. Next I performed mutagenesis studies on USP30 to better understand its mechanism of catalysis. I also strived to obtain recombinant USP30 in high purity and quantity for crystallization screening.

Chapter 2

RESULTS

2.1 Cloning

USP30 has a trans-membrane region spanning the first 56 amino acids of the proteins N-terminal region. The catalytic portion of the enzyme is found in the cytosol and constitutes the remaining amino acids from 57 to 517. The condition used for protein purification is designed to mimic the cytosol of a cell but not the non-polar environment of the mitochondrial membrane. In order to prevent aggregation, and allow for protein solubility, the membrane portion of USP30 was not included. The expression construct was created with a truncated form that did not include the transmembrane (TM) region. Here after all references to the USP30 gene will be referring to the USP30 Δ TM version of the protein.

The vector containing the USP30 Δ TM gene was originally expressed in a Champion pET-SUMO vector. Small Ubiquitin-like Modifier or SUMO could act as a stabilizing protein and increase the solubility of USP30 when expressed in tandem. The SUMO-USP30 recombinant protein was expressed with a His affinity tag in the N-terminal region. Ni-NTA resin was used to pull out the target protein. The SUMO protease ULP1 was then used to cleave off the SUMO tag.

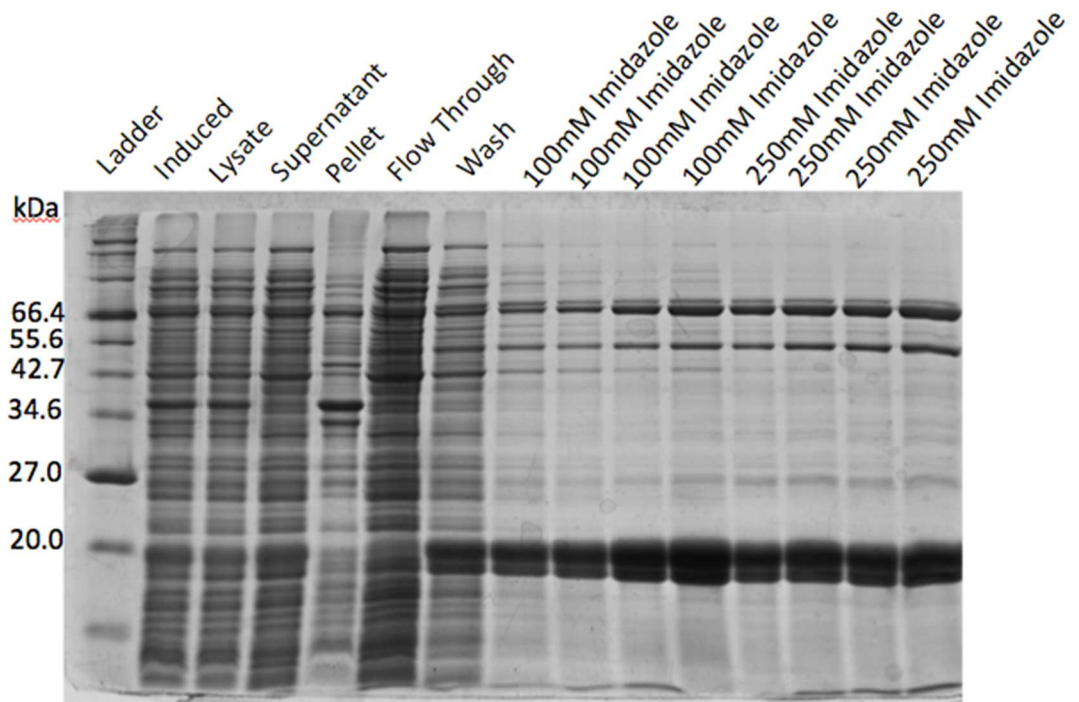


Figure 1 **USP30-SUMO Affinity Purification.** SDS-PAGE analysis of purification using Ni-NTA resin to isolate the His tagged SUMO USP30 protein. The bands in the imidazole elution fraction near 66.4 kDa are SUMO-USP30. The expressed truncated USP30-SUMO can be seen close to 20 kDa.

Although the addition of SUMO was successful in increasing USP30 solubility, the combination resulted in lower than optimal yields. SUMO was shown to be difficult to separate from the target protein during purification. SUMO binds with a greater affinity to anion exchange columns and could be separated from the target protein using ion exchange chromatography. The separation was performed using a HiTrap Q FF column using a NaCl (50 to 600 mM) salt gradient.

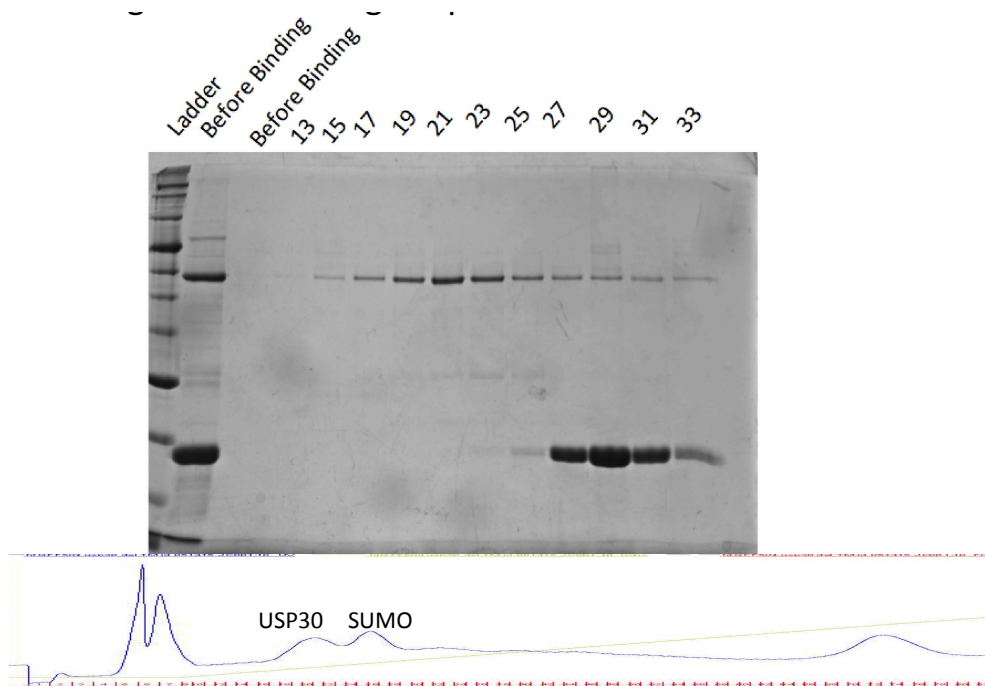


Figure 2 **USP30 Ion Exchange Chromatography:** Top Image: SDS-PAGE page of USP30 separation from SUMO using anion exchange. There is a clear separation between the proteins but a portion of the USP30 can be seen to overlap the SUMO fractions. Bottom Image: Shows the chromatogram of the ion exchange chromatography.

The production of a truncated SUMO-USP30 and the lack of a complete separation during the ion exchange, made the pET-SUMO vector an invalid option. In order to produce USP30 in the amount and purity needed for crystallography studies a new construct would be needed. A modified pET-15b vector with a TEV cleavage site in place of its original thrombin cleavage site was chosen.

Met G S S H H H H H S S G E N L Y F Q G H Met T E R K K R R K G L V P G L V N L G N T
 A F M e t N S L L Q G L S A C P A F I R W L E E F T S Q Y S R D Q K E P P S H Q Y L S L T
 L L H L L K A L S C Q E V T D D E V L D A S C L L D V L R M e t Y R W Q I S S F E E Q D A
 H E L F H V I T S S L E D E R D R Q P R V T H L F D V H S L E Q Q S E I T P K Q I T C R T
 R G S P H P T S N H W K S Q H P F H G R L T S N |

Figure 3 **pET-15b Cloning-Expression Region:** Amino acid sequence translated from DNA sequence results. The His tag is represented in green, the TEV cleavage site is yellow, USP30 sequence is show in blue.

The USP30 gene was extracted from the previous pET-SUMO vector through PCR amplification. The primers used to amplify USP30 gene also introduced the XhoI and NdeI restriction sites. PCR amplification product was then run on a 0.8% agarose gel to separate amplified DNA from other PCR reaction reagents and ensure correct estimated length.

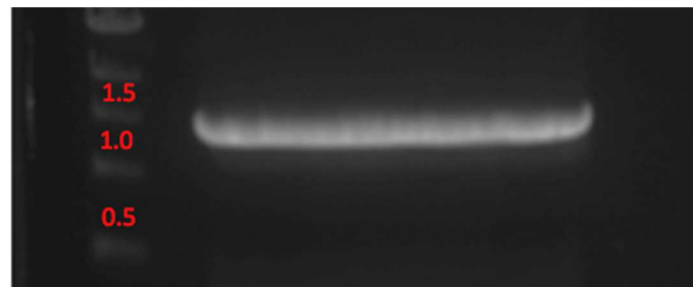


Figure 4 **PCR Amplification Result:** Agarose gel image of the PCR reaction visualized using ethidium bromide. The amplification band is located at the expected length for the 1386 bp USP30 gene.

The band with the correct length was excised and dissolved using Qiagen gel extraction kit. The DNA was then digested with NdeI and XhoI restriction enzymes to produce sticky ends. The restricted gene was then purified using a Qiagen PCR clean up kit before being used for ligation. The modified pET-15b expression vector used

was acquired from Kun Yang and had a previously inserted PCNA gene in the multiple cloning sites. The pET-15b vector was also digested with NdeI and XhoI to give complementary ends for ligation.

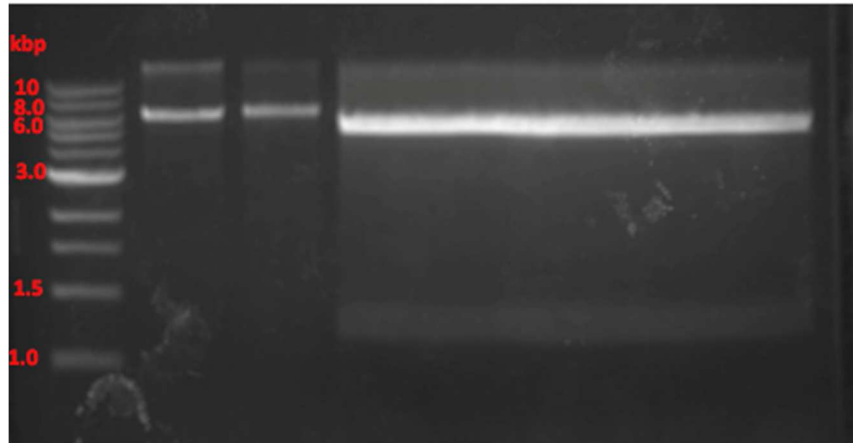


Figure 5 **Double digestion of pET-15b vector:** The first two lanes after the ladder are the single digestion from XhoI and NdeI respectively. The fourth lane is the double digested pET-15b vector. The PCNA gene has been excised and can be seen between 1 and 1.5 kbp markers in the ladder.

Once template vector was digested, the DNA was run on an agarose gel and extracted using the Qiagen gel extraction kit. The USP30 gene was then ligated into the pET-15b vector using the NEB Quick Ligation kit.

The ligation product of the USP30 gene cloned into the modified pET-15b vector was transformed into the high plasmid copy number TOP10 Competent cells. The cells were transferred onto agar plates containing Ampicillin 100 µg/ml as a selection marker.

Multiple colonies were then selected for positive screening by PCR amplification of inserted USP30 gene. Colonies that gave a positive result indicated by a strong amplification band were selected and sent out for DNA sequence verification. DNA was then purified and the transformation of BL21(DE3) cells were performed.

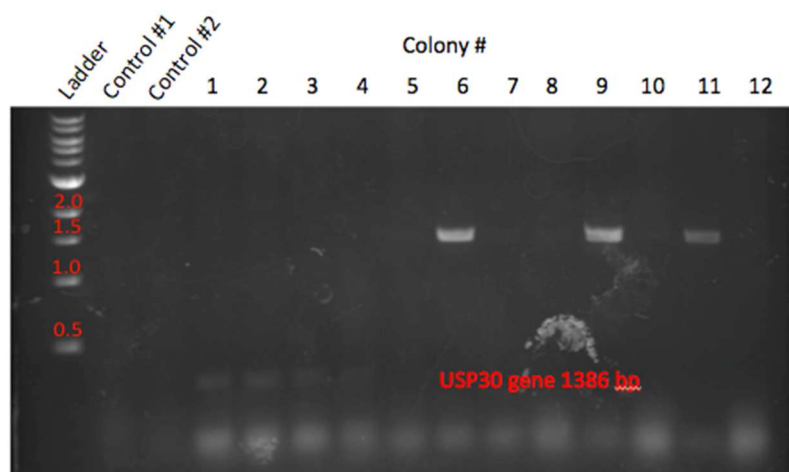


Figure 6 **Gene insertion verification via PCR amplification:** To screen for colonies with the targeted gene inserted, a PCR reaction was performed using primers that would only amplify the USP30 gene. A control of unreacted mixture was run on the gel. Colonies 6, 9, and 11 show a positive result.

2.2 Protein Expression

Once the correct complete gene sequence was verified, the ideal concentration of IPTG for induction of USP30 expression needed to be determined. Because too high an IPTG concentration can be damaging to *E. coli* the lowest effective amount of IPTG is preferable²⁸. Expression testing was performed by growing cells in LB at 37°C till an O.D. of 0.6 was reached. Expression was induced by adding either 0.4 mM or 1 mM IPTG to the cell culture. Samples were taken periodically and the

cultures were left to incubate overnight at 37°C. The amount of cells in the samples were then normalized to assure equal amounts of mass and lysed by heating for 10 min at 100°C before being separated on a 15% SDS PAGE gel. There was a clear amplification of USP30 Δ TM after induction. The induced band is close to the 55 kDa marker of the protein ladder, which is close to the calculated 52.5kDa molecular weight of USP30 Δ TM. The protein amounts expressed by the 0.4 mM IPTG induction is nearly identical to the higher 1 mM concentration.

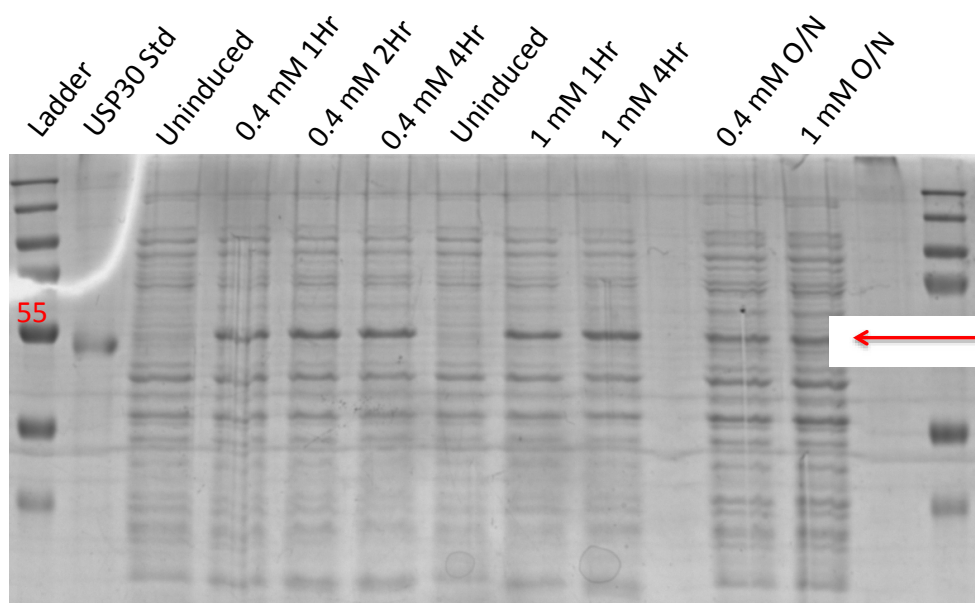


Figure 7 **BL21(DE3) Cells Expression Test:** BL21(DE3) cells transformed with the pET-15b vector containing the USP30 gene were induced using either 0.4 mM or 1 mM IPTG. Samples were taken at various times and analyzed.

2.3 Protein Purification

The first stage of purification is to use the 6X His tag conjugated to USP30 to perform immobilized metal affinity chromatography (IMAC). IMAC using a His tag is usually performed using either nickel (Ni(II)) or cobalt (Co(II)) as the chelating

cation. Attempts using both types of resin revealed that although the target bound stronger to the Ni-NTA, the resulting non-specific binding introduced too many impurities. The loss in overall yield was offset by increasing the mass of cells used for each purification. Co-NTA agarose (Invitrogen) resin gave better overall results. BL21(DE3) cells expressing USP30 were grown in batches 20 Liters of LB with ampicillin. Protein expression was induced with 0.4 mM IPTG. The cells were left to generate protein overnight at 14°C degree and were harvested after 16 hours. The pellet was suspended in Lysis Buffer (50 mM HEPES at pH 7.2, 5 mM β -ME, 10% Glycerol, 10 mM $MgCl_2$, 150 mM NaCl, and 20 mM imidazole). Sample was sonicated to lyse cells. Lysate was centrifuged in Sorval SS-34 rotor for 40 min at 15k RPM. The supernatant was separated from the pellet and incubated with HisPur™ Ni-NTA resin for 1 hour at 4°C. The resin supernatant mixture was then filtered through a gravity column. The resin was washed with a low imidazole solution to remove non specific binding proteins, the protein of interest was eluted using a 40mM, 100mM and 250mM imidazole solution.

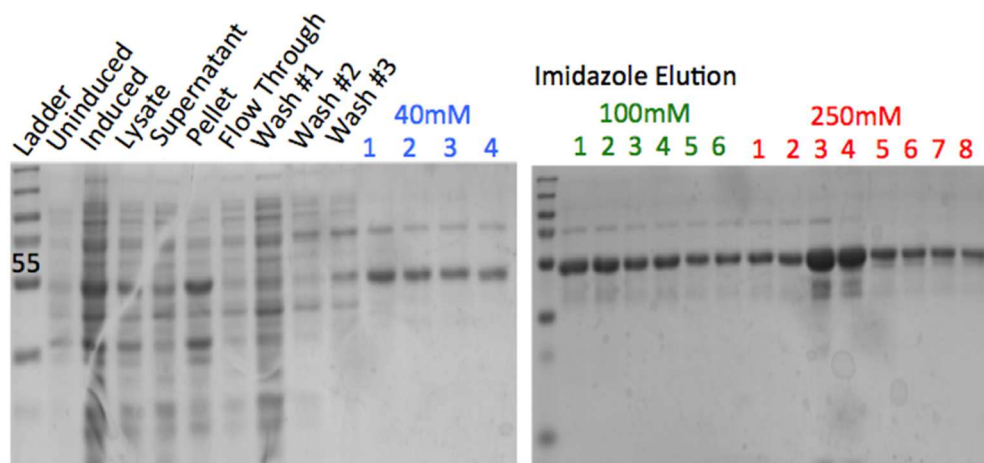


Figure 8 **Analysis of affinity chromatography:** Gel analysis shows a strong band of the target protein after induction. The presence of the target protein in the pellet fraction indicates some of the expressed protein was insoluble along with a major contaminating band. The flow through and wash fractions are relatively free of target protein indicating tight binding between the affinity beads and the target protein. Imidazole elution fractions show a relatively pure sample with an impurity above the target protein.

The next stage in purification was ion exchange chromatography. USP30 has a calculated pI of 7.65. In order to increase affinity of the target protein to an ion exchange column, the buffer pH can either be raised to make the protein negative or lowered causing the protein to become positive. Chromatography using a buffer pH of 8.5 and the anion exchange column of HiTrap Q FF was attempted. The result was that USP30 protein eluted in the flow through with minimal binding of impurities to the column. Better results were achieved by lowering the pH to 6.5 and using the cation exchange column HiTrap SP FF.



Figure 9 **Cation Exchange Chromatography:** Impurities that previously bound to the Ni-NTA resin had the property of carrying a net negative charge. By using a cation exchange column in the next step, many of the impurities did not bind to the column and were present in the flow through fractions.

Before loading on the column a dialysis was performed on the protein. The dialysis served multiple functions. Besides lowering the pH of the solution, it was also necessary to reduce the concentration of imidazole and NaCl. The eluted protein was dialyzed using a 14 kDa molecular weight cutoff Spectra/Por™ dialysis bag. The sample was incubated for 2 hours with minimal stirring in dialysis buffer (2 mM DTT, 50 mM NaCl, 20 mM HEPES pH 7.2, 10% Glycerol). After incubation, TEV protease was added to the sample in a 1:100 ratio and left to cleave over night. It is important to add Tev protease after dialysis since the presence of imidazole acts as an inhibitor to Tev cleavage. Cleavage efficiency and protein identification was performed through mass spectrometry

The sample was then loaded onto the AKTA protein purification system. The strong cation exchange column HiTrap SP was used eluting over a salt gradient of 10-500 mM NaCl. The presence of target protein in elution fractions was determined by SDS-PAGE (figure 2.3.2). Pure fractions were pooled and loaded onto the DuoFlow chromatography system (BioLogic). The final purification step utilized gel filtration. The sample flowed through the Hi-Load 16/60 Superdex 200. This step removed the glycerol from the sample and eluted the protein in its final buffer composition of 1 mM DTT, 20 mM HEPES pH 6.5, 100 mM NaCl. The final purity shown below is high enough for crystallography studies and allows for accurate determination of concentration when used in activity assays.

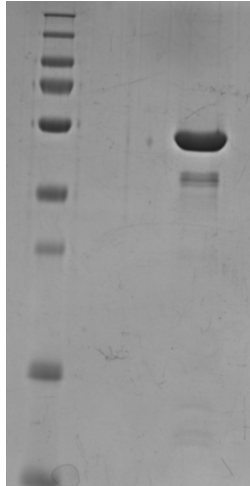


Figure 10 **Final SDS-PAGE analysis of purified USP30 protein:** The resulting protein of the three chromatography methods shows high purity at a concentration of 14 mg/ml.

2.4 Kinetics

Fluorescence spectroscopy was used to determine the steady-state kinetics of USP30. The kinetics analysis was performed through measuring the cleavage rate of the fluorophore 7-amino-4-methylcoumarin(AMC) tagged to C terminus of ubiquitin in the substrate Ub-AMC. AMC has a peak excitation wavelength of 365 nm and a peak emission wavelength of 440 nm. This fluorescence is quenched when bound to ubiquitin. By monitoring the rate of the increase in emission we can calculate the velocity of the reaction.

The Ub-AMC substrate was generated in a multi stage-process. This process was first developed in 2003 to characterize the cleavage of an ubiquitin-like protein (ULP) called NEDD8²⁹. First a truncated ubiquitin 1-75 is expressed in the pTYB1 vector. The expressed vector creates a Ub¹⁻⁷⁵-intein-CBD fusion protein. The recombinant protein is then attached to chitin binding beads under conditions that allow for the rearrangement and subsequent cleavage of the intein sequence from

truncated ubiquitin reaction with MESNA. This creates a highly reactive thioester at the C terminus of the truncated ubiquitin. The thioester can then be reacted with the nucleophilic Glycine-AMC using the catalyst N-hydroxysuccinimide. The resulting Ub-AMC can then serve to be used to track the rate of proteolysis.

For this experiment, a 10 nM concentration of the USP30 Δ TM enzyme was used. The reaction took place in a buffer of 50 mM HEPES at (pH 7.8), 0.5 mM EDTA, 100 mM NaCl, 0.1 mg/ml BSA and 1 mM DTT. The Ub-AMC substrate was tested under varying concentrations (100-5000 nM). Although the cleavage response was still linear at concentrations as high as 5000 nM Ub-AMC, the solubility limit of Ub-AMC prevented the use of high enough substrate concentrations to reliably determine V_{max} . This prevented us from using the standard Michaelis-Menten equation analysis. The kinetic data was instead interpreted using the Lineweaver-Burke linear regression analysis.

$$\frac{1}{V} = \frac{K_M}{V_{max}} \left(\frac{1}{[S]} \right) + \frac{1}{V_{max}}$$

The analysis showed a V_{max} of 3.60 nM/s and a k_{cat}/K_M value of $2.26 \times 10^4 \text{ M}^{-1} \text{ s}^{-1}$ and a relatively high K_M Value of 15.9 μM . These results are consistent with another groups attempt to characterize USP30 kinetic activity in which a k_{cat}/K_m $1.3 \times 10^4 \text{ M}^{-1} \text{ s}^{-1}$ was reported³⁰.

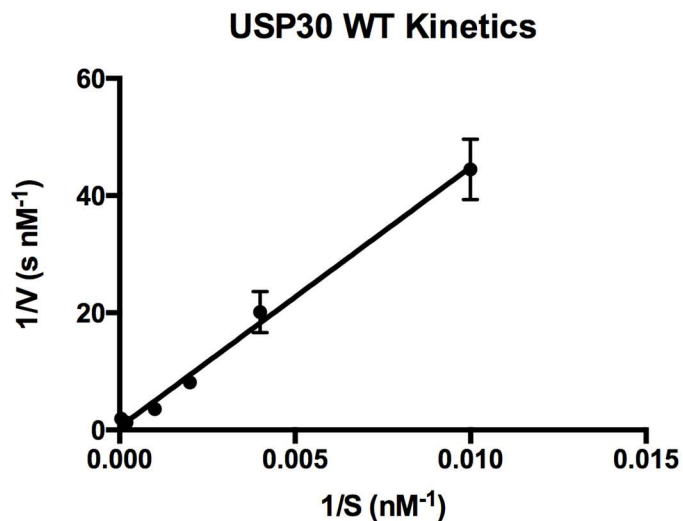


Figure 11 **Lineweaver-Burk Analysis of Wild Type USP30:** Analysis based on the Ub-AMC cleavage fluorescence rate. A k_{cat}/K_M value of $2.26 \times 10^4 \text{ M}^{-1} \text{ s}^{-1}$ was determined.

Site directed mutagenesis was performed on the WT USP30 gene in order to explore the catalytic triad of USP30. USP30 is a cysteine protease with a catalytic triad composed of Cys-His-Ser. The mutations were selected to minimize the effect on the protein folding. Cysteine was mutated to alanine, histidine was changed to glutamine, and serine was change to either alanine or aspartate. Each mutation was introduced using a QuikChange PCR protocol. A representative gel showing the purified USP30 mutants is shown below.

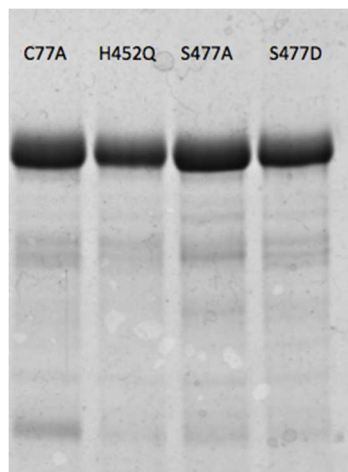


Figure 12 **USP30 Active Site Mutant Purity Assesed SDS –PAGE:** The purity of the mutant (C77A), (H452Q), (S477A), and (S477D) is represented in the gel.

Kinetic analysis as described above was carried out on the individual USP30 mutations. The analysis was also performed using the Lineweaver Burke linear regression. The results showed a loss of activity for the cysteine 77 to alanine and histidine 452 to glutamine mutations. When serine 477 was mutated to alanine there was an estimated 100 fold loss in activity, while an Aspartate mutation resulted in close to 10 fold decrease in catalytic efficiency compared to wild type.

In summary learning from our previous purification attempts we produced a method to generate high yield and purity USP30. A new construct using a pET-15b expression vector was created. Several purification schemes were tested until an optimized version was discovered. The purified protein was then used to characterize the kinetics of USP30 using a florescence-based assay. Mutations of the active site were generated and tested to determine the effects on enzyme activity. Through this method we gain insight into the role of the amino acids that comprise the active site.

Chapter 3

MATERIALS AND METHODS

3.1 DNA Purification

Using aseptic techniques 20 μ L of Ampicillin (100 mg/ml) was added to 20 mL of LB media in a 50 mL tube. A scrape of the Top10 cell stock containing the USP30 Δ TM gene in the pET-SUMO vector was added to the 50mL tube. The cells were then placed inside a shaker incubator at 37°C and left to grow overnight. The cells were then pelleted down by centrifugation at 4,000 RPM for 10 minutes. DNA was extracted using GeneJET Plasmid Miniprep Kit (Thermo Scientific). DNA concentration was determined via the NanoDrop ND-2000 UV-Vis spectrophotometer (Thermo Scientific).

3.2 pET-15b USP30 Vector Creation

The USP30 gene was amplified using PCR. The primers listed below were designed to introduced the restriction sites NdeI and XhoI

USP30 pET-15b NdeI-GGGGTCATATGACAGAAAGAAAGAAGCGTAGAAAAGGG

USP30 pET-15b XhoI- GGTGGTGCTCGAGTTATTCTTCAGACTTGCACTCC

Reaction mixer	(μl)
ddH ₂ O	12.4
5x Buffer	4.0
dNTPs (10mM)	0.4
XhoI Primers (10uM)	1.0
NdeI Primers (10uM)	1.0
Template DNA (25ng/ μ l)	1.0
<u>Phusion DNA polymerase</u>	<u>0.2</u>
Total Volume	20

PCR Program:

Stage	Temp	Time (min)
Initial Denaturation	98°C	00:30
Denaturation	98°C	00:10
Annealing	60°C	00:30
Elongation	70°C	01:15
Cycles		(30)
Final Elongation	72°C	10:00

Samples were then run on 0.8% agarose gel for 40 minutes at 90 V. DNA was then purified from gel using QIAquick Gel Extraction Kit (Qiagen).

ddH ₂ O	60 μ l
Cutsmart 10X Buffer	10 μ l
XhoI	2.5 μ l
NdeI	2.5 μ l
<u>DNA (100 ng/μl)</u>	<u>25 μl</u>
Total Volume	100 μ l

Proteins and DNA fragments removed via PCR clean up using GeneJet PCR Purification Kit (Thermo Scientific). The pET-15b vector was digested using the above protocol. Product was run on agarose gel and purified using QIAquick Gel Extraction Kit (Qiagen).

For the ligation of the USP30 Δ TM gene into the digested pET-15b vector, the NEB Quick Ligation Kit was used. Fifty nanogram of the digested vector DNA was

combined with 3 times the molar concentration of the inserted gene. The reaction mixture is combined and left at room temperature for 5 minutes. The below equation was used to determine appropriate volumes.

$$\frac{(3)(50)(\text{Gene Length})}{(\text{Vector Length})(\text{gene concentration})} = \text{Volume in } \mu\text{l of gene}$$

$$\frac{(3)(50)(\text{USP30}[1386\text{bp}])}{(\text{pET15b}[5708\text{bp}])(\frac{39\text{ng}}{\mu\text{l}})} = 0.94 \mu\text{l of gene}$$

The reaction mixture is combined and left at room temperature for 5 minutes.

Ligation Reaction	(μl)
ddH ₂ O	7.79
2 X Ligation buffer	10
USP30 (39ng/ μl)	0.94
pET-15b (39.5ng/ μl)	1.27
<u>Quick Ligase</u>	<u>1.0</u>
Total Volume	21

3.3 Site directed mutagenesis

The four mutants were created by the use of primers listed below introducing a single point mutation. The PCR was generated using the method described above.

The template DNA was then digested with DpnI and the mutant plasmid transformed into TOP10 cells.

Primer Sequence

USP30 C146A F CTTGTTAATTTAGGGAACACCGCCTTCATGAACTCCCTGC
USP30 C146A R GCAGGGAGTTCATGAAGGCGGTGTTCCCTAAATTAACAAG
USP30 H521Q F CATGGAGACATGCACTCTGGACAATTTGTCACTTACCGAC
USP30 H521Q R GTCGGTAAGTGACAAATTGTCCAGAGTGCATGTCTCCATG
USP30 S546A F CTAGCAATCAGTGGCTGTGGGTCGCCGATGACACTGTCCG
USP30 S546A R CGGACAGTGCATCGGCGACCCACAGCCACTGATTGCTAG

3.4 Transformation Procedure

Typical heat shock transformation protocol was utilized. Tubes of desired cell line [Top10 or BL21(DE3)] were thawed on ice. Once thawed 2 μ l of purified DNA was added to the tube and left to incubate for 45 min. Cells were then placed in a hot water bath of 42°C for 45 seconds and then placed on ice for 2 mins. Then 350 μ l of SOC media was added to mixture and tubes were incubated in a shaker at 37°C for 1 hour. Cell mixture was then added to LB plates containing Ampicillin and incubated overnight.

3.5 Sequencing

The sequencing for all constructs was performed by GENEWIZ[®] and results were analyzed to determine quality and accuracy of results using CLC Sequence viewer 7 software.

3.6 Expression test

First 50 ml tubes were filled with 15ml of LB + 100 μ g/ml Ampicillin. Colonies of BL21(DE3) cells containing the USP30 gene inserted into the pET-15b plasmid were added to the LB mixture. Once OD_{600nm} levels reached 0.6 samples were induced with 0.4 mM IPTG and left to shake over night at 37°C. Protein expression levels were then determined using SDS-PAGE.

3.7 BL21(DE3) cell cultivation and harvesting

High protein expressing colonies were incubated overnight at 37°C. These cell were used to inoculate shaker flask containing 4 L of LB +100 mg/L Amplicilin. Flasks are incubated in a shaker at 37°C. Once O.D. of 0.4 was reached the temperature was dropped to 17°C and O.D. was observed every 20 minutes till reaching 0.6 at which time 0.4 mM IPTG was added to induce protein expression. Cells were left to shake over night. Cells were harvested by centrifugation at 5000 RPM for 10 mins.

3.8 Stage 1 purification

Cell pellet was weighed in suspended in lysis buffer(50 mM HEPES at pH 7.2, 150 mM NaCl, 10 mM MgCl₂, 10% glycerol, 5 mM β-ME, 20 mM imidazole, and 0.1% Triton X-100) in a concentration of 10 ml/g. Sonication was used to disrupt cell membrane. Sonicator was set to duty cycle 5, output 8 and warmed up for 30 minutes. Lysis solution was chilled in ice slurry bath. Probe was lowered about 2/3 towards the bottom of suspended cells. Cells were sonicated on/off for 30-second intervals for a duration of 30 min in 100 ml batches. Cell lysate was centrifuged for 40 minutes at 15,000 RPM. Ni-NTA Agarose nickel resin was washed twice with ddH₂O and twice with lysis buffer. Supernatant was removed from pelleted cell debris and incubated with equilibrated Ni-NTA resin. The incubation takes place in a 4°C cold room for one hour, with the samples being continuously rotated. The resin beads bound to the target protein are loaded onto a gravity column and the supernatant is allowed to flow through a filter. The non-specific binding proteins are then washed away with additional lysis buffer. The target protein is then eluted in 5 ml collection volumes

using 50 ml each of a 40 mM, 100 mM, and a 250 mM imidazole solution. Samples from each stage of the purification and eluted fractions were run on 15% SDS-PAGE for 60 min at 200V

3.9 Stage 2 Purification

Fractions showing purified protein were pooled and dialyzed. Protein concentrations of pooled fractions were determined using the Bradford Protein Assay by Bio-Rad^l. A 1:100 molar ratio of Tev protease was added to the mixture to cleave His tag from target protein during dialysis. Cleavage was verified by both SDS-PAGE and mass spectrometry. The eluted protein was dialyzed using a 14KD Molecular weight cut off Spectra/PorTM dialysis bag. Dialysis was performed in 4°C cold room using lowest stirring speed setting. 2 liters of buffer were used and solution was changed ever hour for 2 hours. Dialysis buffer consist of 2 mM DTT, 50 mM NaCl, 20 mM Hepes, 10% Glycerol, pH 6.5. Sample loaded onto HiTrap SP column using the Akta protein purification FPLC. Proteins eluted over a 0.5 M NaCl gradient, with fractions showing strong UV 280 nm absorption being collected and examined using SDS-PAGE.

3.10 Stage 3 Purification

Positive fractions where then concentrated down to 1ml volume using Pierce Protein Concentrators with a 10K molecular weight cut off. A series of 1:1 buffer exchanges were used during concentration to acclimate the proteins to the conditions of the size exclusion purification. The buffer used was the same as the running buffer

for the size exclusion, a buffer containing 20 mM hepes 7.2, 150 mM NaCl, and 1 mM DTT. The concentrated protein was loaded onto a Hiload 16/60 Superdex 200 column (GE Life Science). Final purity of the protein was eluted through SDS-PAGE and mass spectrometry.

3.11 UB-AMC production

The sequence for Ub₁₋₇₅ was placed in an intein fusion vector and expressed in BL21(DE3) cells. The cells were grown and harvested as detailed previously.

The harvested cells were suspended in lysis buffer: 20mM Tris (pH 7.5), 200nM NaCl, 5% Glycerol, 1mM EDTA. Cells were then sonicated and centrifuged. The supernatant was incubated with chitin beads for four hours in a 4°C cold room. The beads are first washed with a high salt buffer: 20mM Tris (pH 7.5), 500nM NaCl, 5% Glycerol, 1mM EDTA followed by a low salt wash: 20mM MES(pH 6.5), 100mM NaCl. To cleave the target protein, the chitin beads were incubated with a buffer containing 75 mM MESNA. The Ub-MESNA was then concentrated down to 3 mg/ml and buffer exchanged with a 50 mM NaH₂PO₄ solution. A reaction mixture of Nhydroxysuccinimide (5 mg/mL), collidine (20 mg/mL), glycine-AMC (10 mg/mL), and 20% dimethyl is added to the concentrated Ub-MESNA. The mixture is then rotated at room temperature for 40 hours. The conjugated Ub-AMC product is then purified via HPLC reverse phase chromatography.

3.12 Kinetics

Enzyme kinetic characterization took place at room temperature in a buffer containing 50 mM HEPES (pH 7.8), 0.5 mM EDTA, 0.1 mg/mL BSA, 1 mM DTT and 100mM NaCl at 25 °C. Rate of cleavage was measured by change of fluorescence using a Fluoromax-4 fluorescence spectrometer (Horiba) . The emission wavelength used is 440 nm and the excitation wavelength is 355 nm.

Chapter 4

DISCUSSION

The mutant kinetic analysis confirms the location and function of the active site cysteine and histidine. The mutational analysis also highlights the important role of serine in the cleavage mechanism. The serine to aspartate mutation resulted in a ten-fold decrease in enzyme activity. Aspartate and serine share a similar structure substituting the hydroxyl found in serine for the carboxyl found in aspartate. If the hydroxyl group is removed entirely as was the case in the alanine mutation there is an approximately 100 fold decrease in enzyme activity. Of the more than 50 USPs in humans, only three share the Cys-His-Ser triad; USP30, USP16, and USP45. This uniqueness has the potential to be exploited when developing a specific inhibitor for USP30.

Using the new plasmid design and the optimized purification method, I was able to extract a total of 21 mg of > 95% pure USP30 protein. The molecular weight was verified by mass spec analysis. This method is efficient and could provide the substrate needed for many *In vitro* experiments. While the importance of USP30's role in mitophagy is well documented, currently only a handful of significant studies have been performed on the purified USP30 enzyme. A group at the Tokyo Institute of Technology was able to isolate both the wild type and a cysteine to serine mutate. However, their analysis of the enzyme kinetics was entirely gel based and did not provide rigorous quantitative analysis³¹. In 2014 another group announced a small molecule inhibitor of USP30 was isolated, named diterpenoid derivative 15-

oxospiramilactone (S3)³². The small molecule S3 was shown to increase fusion through decreased degradation of Mfn1 and Mfn2. The bulk of the data acquired by the group was through cell visualization and western blot analysis. Again the analysis performed on the purified USP30 was through gel analysis, displaying the cleavage of tetra-ubiquitin in the presence varying concentration of inhibitor. A recent publication in nature by Genentech has the most complete analysis of purified USP30 to date²⁶. The group performed a fluorescence based kinetic analysis similar to the technique in this thesis. They also reported experiencing difficulty achieving saturation due to the solubility of Ub-AMC. In the publication the group tested USP30 cleavage rate against different chain linkages, noting that USP30 had the highest preference for the irregular K6 chain linkage. This information correlates well with their observation that K6 linkages are increased by Parkin during membrane depolarization. These findings leave room for further experiments that can quantify the cleavage rate of USP30 using a compact chain substrate. This may increase the binding affinity for the substrate and lower the K_m allowing for Michaelis Menten analysis.

Although crystal structure exists for Parkin³³, as of yet there are no crystal structures of the USP30 enzyme. A crystal structure of USP30 would open the door to many more important avenues of research. The structure would allow for more accurate molecular modeling, which is particularly useful when using software that attempts to predict binding interactions between the protein and the ligand.

All of these avenues could help create a much-needed alternative to the currently existing treatment for Parkinson's. Treatment falls into mainly two categories. Either the administration of a dopamine precursors like Levodopa which can pass the blood brain barrier before being converted to dopamine or a dopamine

agonist like Mirapex which mimics the effects of the dopamine molecule³⁴. Neither of these options protects the cell from damage or reverses the disease. The current cost of Parkinson's care will be overshadowed by the rising cost of care that comes with our aging population. The number of Alzheimer's patients is expected to double by the year 2050³⁵. It is estimated that the current total cost to treat the top 9 neurological disorders is close to 800 billion in the US. That is over 100 million more than defense spending. A line of research, which could restore healthy mitochondrial networks in dopamine producing cells, could be of invaluable benefit in the coming years.

REFERENCES

1. “Parkinson's Disease Foundation (PDF) Hope through Research, Education and Advocacy, 21 June 2017, www.pdf.org/.
2. Johnson, S., Diener, M., Kaltenboeck, A., Birnbaum, H., & Siderowf, A. (2013). An economic model of Parkinson's disease: Implications for slowing progression in the United States. *Movement Disorders*, 28(3), 319-326. <http://dx.doi.org/10.1002/mds.25328>
3. Goetz, C. (2011). The History of Parkinson's Disease: Early Clinical Descriptions and Neurological Therapies. *Cold Spring Harbor Perspectives In Medicine*, 1(1), a008862-a008862. <http://dx.doi.org/10.1101/cshperspect.a008862>
4. Trinh, J., & Farrer, M. (2013). Advances in the genetics of Parkinson disease. *Nature Reviews Neurology*, 9(8), 445-454. <http://dx.doi.org/10.1038/nrneuro.2013.132>
5. Goetz, C. (2011). The History of Parkinson's Disease: Early Clinical Descriptions and Neurological Therapies. *Cold Spring Harbor Perspectives In Medicine*, 1(1), a008862-a008862. <http://dx.doi.org/10.1101/cshperspect.a008862>
6. Zhou, J., Broe, M., Huang, Y., Anderson, J., Gai, W., & Milward, E. et al. (2011). Changes in the solubility and phosphorylation of α -synuclein over the course of Parkinson's disease. *Acta Neuropathologica*, 121(6), 695-704. <http://dx.doi.org/10.1007/s00401-011-0815-1>
7. Cookson, M. (2009). α -Synuclein and neuronal cell death. *Molecular Neurodegeneration*, 4(1), 9. <http://dx.doi.org/10.1186/1750-1326-4-9>
8. Petrucelli, L., O'Farrell, C., Lockhart, P., Baptista, M., Kehoe, K., & Vink, L. et al. (2002). Parkin Protects against the Toxicity Associated with Mutant α -Synuclein. *Neuron*, 36(6), 1007-1019. [http://dx.doi.org/10.1016/s0896-6273\(02\)01125-x](http://dx.doi.org/10.1016/s0896-6273(02)01125-x)

9. Sitia, R., & Braakman, I. (2003). Quality control in the endoplasmic reticulum protein factory. *Nature*, *426*(6968), 891-894. <http://dx.doi.org/10.1038/nature02262>
10. Nakka, V., Gusain, A., & Raghubir, R. (2009). Endoplasmic Reticulum Stress Plays Critical Role in Brain Damage After Cerebral Ischemia/Reperfusion in Rats. *Neurotoxicity Research*, *17*(2), 189-202. <http://dx.doi.org/10.1007/s12640-009-9110-5>
11. Remondelli, P., & Renna, M. (2017). The Endoplasmic Reticulum Unfolded Protein Response in Neurodegenerative Disorders and Its Potential Therapeutic Significance. *Frontiers In Molecular Neuroscience*, *10*. <http://dx.doi.org/10.3389/fnmol.2017.00187>
12. Geisler, S., Holmström, K., Treis, A., Skujat, D., Weber, S., & Fiesel, F. et al. (2010). The PINK1/Parkin-mediated mitophagy is compromised by PD-associated mutations. *Autophagy*, *6*(7), 871-878. <http://dx.doi.org/10.4161/auto.6.7.13286>
13. Goswami, P., Joshi, N., & Singh, S. (2017). Neurodegenerative signaling factors and mechanisms in Parkinson's pathology. *Toxicology In Vitro*, *43*, 104-112. <http://dx.doi.org/10.1016/j.tiv.2017.06.008>
14. Lin, M., & Beal, M. (2006). Mitochondrial dysfunction and oxidative stress in neurodegenerative diseases. *Nature*, *443*(7113), 787-795. <http://dx.doi.org/10.1038/nature05292>
15. Bingol, B., Tea, J., Phu, L., Reichelt, M., Bakalarski, C., & Song, Q. et al. (2014). The mitochondrial deubiquitinase USP30 opposes parkin-mediated mitophagy. *Nature*, *510*(7505), 370-375. <http://dx.doi.org/10.1038/nature13418>
16. Glauser, L., Sonnay, S., Stafa, K., & Moore, D. (2011). Parkin promotes the ubiquitination and degradation of the mitochondrial fusion factor mitofusin 1. *Journal Of Neurochemistry*, *118*(4), 636-645. <http://dx.doi.org/10.1111/j.1471-4159.2011.07318.x>
17. Birsa, N., Norkett, R., Wauer, T., Mevissen, T., Wu, H., & Foltynie, T. et al. (2014). Lysine 27 Ubiquitination of the Mitochondrial Transport Protein Miro Is Dependent on Serine 65 of the Parkin Ubiquitin Ligase. *Journal Of Biological Chemistry*, *289*(21), 14569-14582. <http://dx.doi.org/10.1074/jbc.m114.563031>

18. Abdul Rehman, S., Kristariyanto, Y., Choi, S., Nkosi, P., Weidlich, S., & Labib, K. et al. (2016). MINDY-1 Is a Member of an Evolutionarily Conserved and Structurally Distinct New Family of Deubiquitinating Enzymes. *Molecular Cell*, *63*(1), 146-155.
<http://dx.doi.org/10.1016/j.molcel.2016.05.009>
19. Youle, R., & van der Bliek, A. (2012). Mitochondrial Fission, Fusion, and Stress. *Science*, *337*(6098), 1062-1065.
<http://dx.doi.org/10.1126/science.1219855>
20. Valente, E. (2004). Hereditary Early-Onset Parkinson's Disease Caused by Mutations in PINK1. *Science*, *304*(5674), 1158-1160.
<http://dx.doi.org/10.1126/science.1096284>
21. Shimizu, N., Kitada, T., Asakawa, S., Hattori, N., Matsumine, H., & Yamamura, Y. et al. (1998). *Nature*, *392*(6676), 605-608.
<http://dx.doi.org/10.1038/33416>
22. Yamano, K., Matsuda, N., & Tanaka, K. (2016). The ubiquitin signal and autophagy: an orchestrated dance leading to mitochondrial degradation. *EMBO Reports*, *17*(3), 300-316.
<http://dx.doi.org/10.15252/embr.201541486>
23. Bingol, B., & Sheng, M. (2016). Mechanisms of mitophagy: PINK1, Parkin, USP30 and beyond. *Free Radical Biology And Medicine*, *100*, 210-222. <http://dx.doi.org/10.1016/j.freeradbiomed.2016.04.015>
24. Kane, L., Lazarou, M., Fogel, A., Li, Y., Yamano, K., & Sarraf, S. et al. (2014). PINK1 phosphorylates ubiquitin to activate Parkin E3 ubiquitin ligase activity. *The Journal Of Cell Biology*, *205*(2), 143-153.
<http://dx.doi.org/10.1083/jcb.201402104>
25. Kondapalli, C., Kazlauskaitė, A., Zhang, N., Woodroof, H., Campbell, D., & Gourlay, R. et al. (2012). PINK1 is activated by mitochondrial membrane potential depolarization and stimulates Parkin E3 ligase activity by phosphorylating Serine 65. *Open Biology*, *2*(5), 120080-120080.
<http://dx.doi.org/10.1098/rsob.120080>
26. Cunningham, C., Baughman, J., Phu, L., Tea, J., Yu, C., & Coons, M. et al. (2015). USP30 and parkin homeostatically regulate atypical ubiquitin chains on mitochondria. *Nature Cell Biology*, *17*(2), 160-169.
<http://dx.doi.org/10.1038/ncb3097>

27. Wang, Y., Serricchio, M., Jauregui, M., Shanbhag, R., Stoltz, T., & Di Paolo, C. et al. (2015). Deubiquitinating enzymes regulate PARK2-mediated mitophagy. *Autophagy*, *11*(4), 595-606. <http://dx.doi.org/10.1080/15548627.2015.1034408>
28. Baneyx, F. (1999). Recombinant protein expression in *Escherichia coli*. *Current Opinion In Biotechnology*, *10*(5), 411-421. [http://dx.doi.org/10.1016/s0958-1669\(99\)00003-8](http://dx.doi.org/10.1016/s0958-1669(99)00003-8)
29. Gan-Erdene, T., Nagamalleswari, K., Yin, L., Wu, K., Pan, Z., & Wilkinson, K. (2003). Identification and Characterization of DEN1, a Deneddylase of the ULP Family. *Journal Of Biological Chemistry*, *278*(31), 28892-28900. <http://dx.doi.org/10.1074/jbc.m302890200>
30. Cunningham, C., Baughman, J., Phu, L., Tea, J., Yu, C., & Coons, M. et al. (2015). USP30 and parkin homeostatically regulate atypical ubiquitin chains on mitochondria. *Nature Cell Biology*, *17*(2), 160-169. <http://dx.doi.org/10.1038/ncb3097>
31. Nakamura, N., & Hirose, S. (2008). Regulation of Mitochondrial Morphology by USP30, a Deubiquitinating Enzyme Present in the Mitochondrial Outer Membrane. *Molecular Biology Of The Cell*, *19*(5), 1903-1911. <http://dx.doi.org/10.1091/mbc.e07-11-1103>
32. Yue, W., Chen, Z., Liu, H., Yan, C., Chen, M., & Feng, D. et al. (2014). A small natural molecule promotes mitochondrial fusion through inhibition of the deubiquitinase USP30. *Cell Research*, *24*(4), 482-496. <http://dx.doi.org/10.1038/cr.2014.20>
33. Wauer, T., & Komander, D. (2013). Structure of the human Parkin ligase domain in an autoinhibited state. *The EMBO Journal*, *32*(15), 2099-2112. <http://dx.doi.org/10.1038/emboj.2013.125>
34. *Parkinson's disease Treatments and drugs*. (2017). *Mayo Clinic*. from <http://www.mayoclinic.org/diseases-conditions/parkinsons-disease/basics/treatment/con-20028488>
35. Gooch, C., Pracht, E., & Borenstein, A. (2017). The burden of neurological disease in the United States: A summary report and call to action. *Annals Of Neurology*, *81*(4), 479-484. <http://dx.doi.org/10.1002/ana.24897>